International Core Journal of Engineering Volume 12 Issue 4, 2026
ISSN: 2414-1895 DOI: 10.6919/ICJE.202604_12(4).0044

Phosphoric Acid-assisted Structural Engineering of Wheat Straw-derived Hard Carbon for High-performance Sodium-ion Batteries

Qian Liu[1, a], Dandan Ma[1, b], Yefeng Feng[2, c], and Miao He[3, d]

[1] School of Physics and Optoelectronic Engineering, Guangdong University of Technology, Guangzhou 510000, China

[2] Guangzhou Qingbei Intelligent Technology Co., Ltd., Guangzhou, 510080, China

[3] The State Key Laboratory of Precision Electronic Manufacturing Technology and Equipment, School of Electromechanical Engineering, Guangdong University of Technology, Guangzhou, 510006, China

[a]514759187@qq.com, [b]2637354676@qq.com, [c]fengyefeng_1001@163.com, [d]herofate666@126.com

Abstract

This article uses agricultural waste straw as a precursor, first employing phosphoric acid pretreatment to regulate its lignocellulosic structure, and prepared phosphoric acid-treated straw hard carbon (PLHC-P). Structural characterization indicates that PLHC possesses a relatively high number of surface oxygen-containing functional groups and defects, with sodium storage primarily occurring through surface adsorption. Phosphoric acid pretreatment effectively deconstructs the dense lignocellulosic structure of straw, creating a rich porous structure through etching, expanding the interlayer spacing of carbon, and introducing phosphorus doping. After further compositing with asphalt, a stable carbon layer is formed, effectively buffering volume changes, further expanding interlayer spacing, increasing closed pore volume, and forming a denser carbon structure. Electrochemical test results show: PLHC has a reversible capacity of 230 mAh/g at a current density of 20 mA/g; PLHC-P has a capacity of 280 mAh/g under the same conditions, and at a high current density of 300 mA/g, PLHC-P maintains a capacity of 200 mAh/g after 800 cycles.

Keywords

Sodium-ion Battery; Wheat Straw; Anode Material.

1. Introduction

With the growth of the population, the demand for energy has greatly increased. The large-scale use of fossil fuels has put the environment under severe pressure [1, 2]. Compared to lithium, sodium is widely available in nature and offers enhanced safety characteristics, making it an attractive candidate for next-generation energy storage systems [3, 4]. Among various anode materials, hard carbon stands out due to its high specific capacity, low operating potential, and sustainable precursor sources [5, 6]. However, there are still some issues that need to be resolved in the practical application of hard carbon anodes, including relatively low initial Coulombic efficiency, insufficient rate capability, and limited plateau capacity, which is critical for achieving high energy density [7, 8].

The low-voltage plateau capacity (< 0.1 V), originating from Na^+ intercalation into pseudo-graphitic layers, influence the overall reversible capacity [11, 12]. Therefore, rational design of precursor

ISSN: 2414-1895 DOI: 10.6919/ICJE.202604_12(4).0044

materials and optimization of carbonization conditions are essential to tailor these structural parameters toward superior sodium storage [9, 10].

Biomass-derived hard carbons have attracted considerable attention due to their renewability, natural abundance, and unique inherent structures [13, 14]. Wheat straw, as an abundant agricultural residue, is particularly attractive because of its high cellulose content and natural fibrous structure, which can potentially facilitate ion transport [15]. Nevertheless, direct carbonization of raw wheat straw typically yields hard carbon with limited closed porosity and insufficient plateau capacity, due to the tight lignocellulosic structure that hinders the formation of favorable pore architectures [16].

Chemical pretreatment of biomass precursors can effectively modulate the microstructure [17, 18]. In particular, phosphoric acid has been shown to deconstruct the lignocellulosic matrix by hydrolyzing cellulose into smaller saccharides and etching the rigid structures of lignin and hemicellulose, thereby promoting the formation of abundant pores and introducing heteroatom doping [19, 20]. Inspired by these findings, we propose a simple phosphoric acid pretreatment strategy to regulate the microstructure of wheat straw-derived hard carbon for enhanced sodium storage performance.

In this paper, we studied the effects of phosphoric acid on the structural evolution and electrochemical performance of wheat straw. The optimized sample, carbonized at 1500 ℃ after phosphoric acid pretreatment, exhibits significantly enhanced reversible capacity, rate capability, and cycling stability compared to the pristine sample.

2. Materials Preparation

Wash the wheat straw thoroughly with deionized water, dry it in an 80℃ oven for 24 hours, and then crush it. Mix the wheat straw powder with 85% phosphoric acid at a mass ratio of 4:1 and ball mill for 12 hours. Pre-carbonize the mixture at 600℃ for 3 hours, then wash it with 1 M HCl at 60℃ for 24 hours to remove inorganic impurities, rinse with deionized water until neutral, and dry. Finally, heat to 1500℃ at a rate of 2℃/min and hold for 2 hours to obtain phosphoric acid-treated wheat straw hard carbon, named PLHC-P. For comparison, the pristine (PLHC) was prepared under identical conditions without phosphoric acid pretreatment.

3. Results and Analysis

3.1 Structural Characterization

The prepared hard carbon samples were studied using XRD. As shown in Fig. 1, both PLHC and PLHC-P exhibit two broad diffraction peaks [21, 22]. These peaks confirm the typical hard carbon structure, featuring abundant structural defects.

Notably, a careful comparison reveals that comparison shows that the (002) peak of PLHC-P is slightly broader. According to the Bragg equation, the interlayer spacing of the PLHC-P sample is greater than that of the PLHC sample, while the pristine PLHC shows a smaller interlayer spacing of about 0.372 nm. This expanded interlayer spacing in PLHC-P is beneficial for facilitating Na^+ intercalation and deintercalation, as the larger d-spacing reduces the diffusion barrier for sodium ions [11, 23]. The observed increase in interlayer spacing can be attributed to the phosphorus doping introduced during phosphoric acid pretreatment, which causes the carbon layers to expand [19, 24].

Furthermore, the (002) peak of PLHC-P is larger, indicating that its structure is more disordered. This is consistent with the phosphoric acid-induced deconstruction of the lignocellulosic structure, which prevents excessive graphitization and preserves abundant defects and active sites for sodium storage [25, 26]. Importantly, no additional sharp peaks corresponding to crystalline impurities are observed in either pattern, confirming the high purity of both carbon materials.

ISSN: 2414-1895 DOI: 10.6919/ICJE.202604_12(4).0044

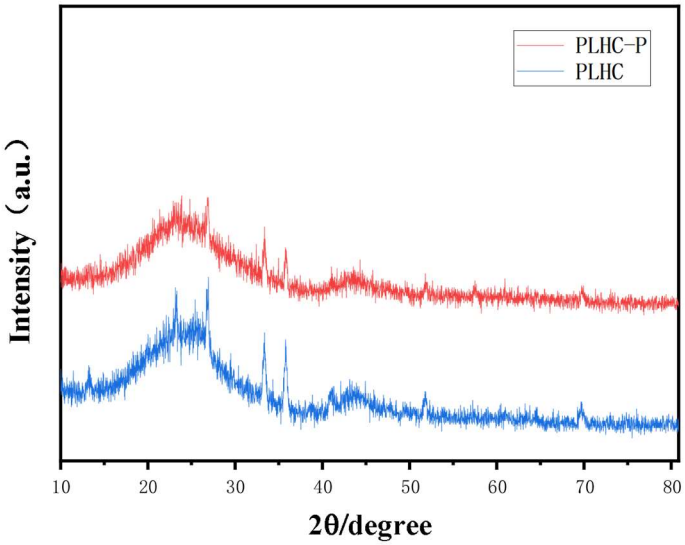

Fig. 1 XRD of PLHC-P and PLHC

Tested by XPS. Fig. 2 and 3 present the high-resolution C 1s and O 1s spectra of PLHC and PLHC-P. The C 1s spectrum of both samples can be deconvoluted into three main peaks: a dominant peak at 284.8 eV corresponding to sp^2/sp^3 hybridized carbon , a peak at 286.2 eV attributed to carbon singly bonded to oxygen [27, 28]. Notably, compared to pristine PLHC, the PLHC-P sample exhibits a slightly reduced intensity of oxygen-containing functional groups, particularly the C–O and C=O peaks, suggesting that phosphoric acid pretreatment partially removes surface oxygen groups.

The O 1s spectra further corroborate this observation. For PLHC, the O 1s spectrum shows peaks at approximately 531.8 eV and 533.2 eV [29]. In contrast, the PLHC-P sample displays an additional peak at around 534.5 eV[30]. This is consistent with the observation that phosphoric acid not only etches the lignocellulosic structure but also serves as a dopant, introducing heteroatoms that may enhance the electrochemical activity [19]. The XPS results confirm that phosphoric acid treatment effectively modulates the surface chemistry of wheat straw-derived hard carbon by reducing oxygen-containing functional groups and introducing phosphorus doping. The reduced oxygen content is beneficial for improving the initial Coulombic efficiency by minimizing irreversible side reactions during the initial sodiation process[31].

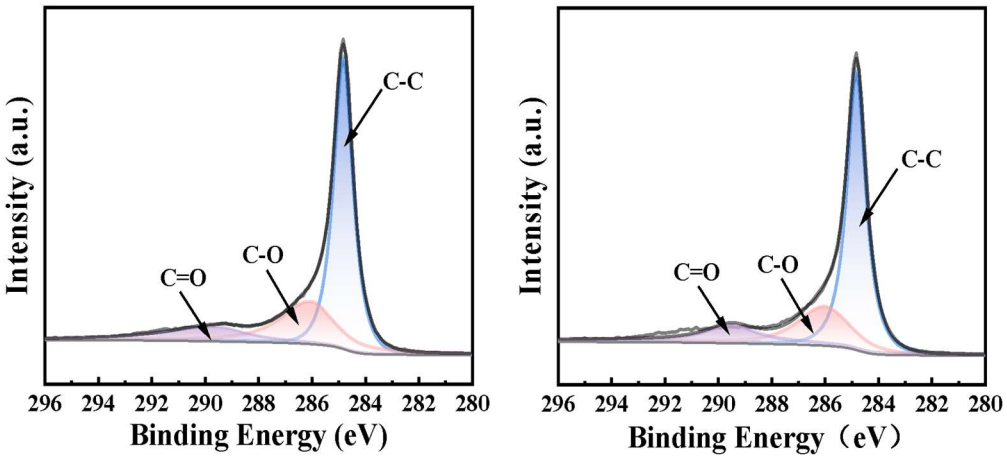

Fig. 2 C Test in XPS of PLHC and PLHC-P

ISSN: 2414-1895 DOI: 10.6919/ICJE.202604_12(4).0044

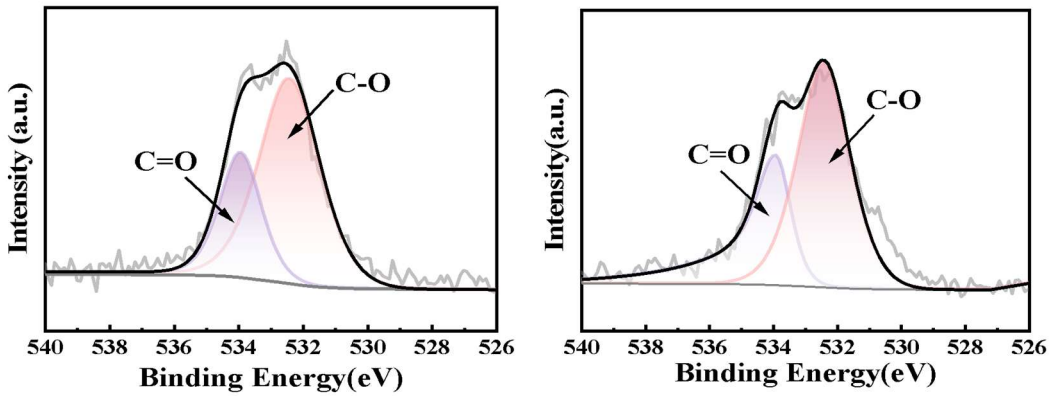

Fig. 3 O test in XPS of PLHC and PLHC-P

3.2 Electrochemical Performance

First, the sodium storage performance of the straw-derived hard carbon anode was evaluated in a half-cell at a low current density of 20 mA g^{-1} to assess its intrinsic reversible capacity and cycling stability. Figure 3-6 shows the cycling performance of PLHC and PLHC-P over 100 cycles. It is worth noting that the PLHC-P anode provided a significantly higher initial reversible capacity of 290 mAh g^{-1}, whereas the original PLHC anode had 190 mAh g^{-1}. More importantly, after 100 cycles, the PLHC-P anode maintained a stable capacity of about 285 mAh g^{-1}, corresponding to a capacity retention of 98.3%, while the PLHC anode only maintained 185 mAh g^{-1} with a retention rate of 97.4%. The superior capacity of PLHC-P throughout the cycling process clearly demonstrates the beneficial effect of phosphate pre-treatment.

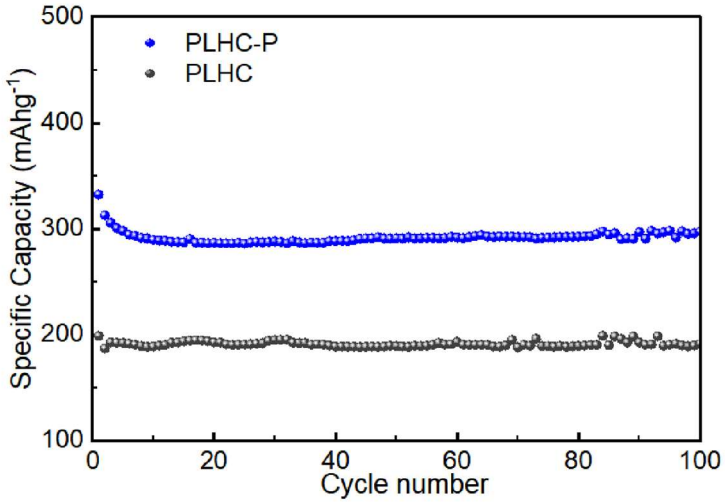

Fig. 4 Cycling performance at 20 mA g^{-1}.

As shown in Figure 4, the PLHC-P electrode exhibited excellent cycling stability over 800 cycles. The initial discharge capacity reached 280 mAh g^{-1}, and after 800 cycles, it still maintained a reversible capacity of 260 mAh g^{-1}, corresponding to a high capacity retention of 92.9%. It is noteworthy that the Coulombic efficiency quickly approached 100% after the first few cycles and remained above 99.5% throughout the cycles, indicating highly reversible sodium insertion/extraction and the formation of a stable solid electrolyte interphase [32, 33].

ISSN: 2414-1895 DOI: 10.6919/ICJE.202604_12(4).0044

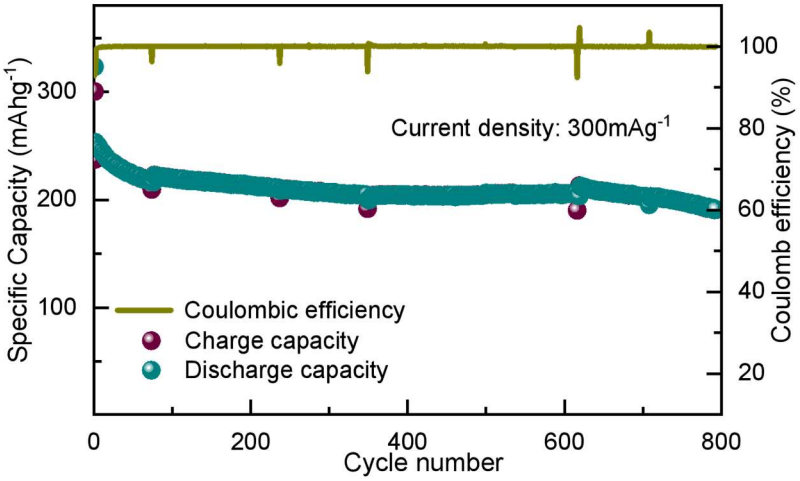

Fig. 5 Cycling performance at 300 mA g^{-1}.

As shown in Fig. 6. At a low current density of 20 mA g^{-1}, PLHC-P delivers a high reversible capacity of 290 mAh g^{-1}, significantly higher than the 220 mAh g^{-1} achieved by the pristine PLHC anode. At current densities of 50, 100, 200, and 300 mA g^{-1}, the PLHC-P anode maintains capacities of 260,240,215, and 200 mAh g^{-1}. In contrast, the PLHC anode shows much lower capacities of 195, 185, 170, and 165 mAh g^{-1} under the same current densities. Notably, when the current density is reduced back to 20 mA g^{-1}, the PLHC-P anode recovers a capacity of 290 mAh g^{-1}, demonstrating great reversibility and structural robustness.

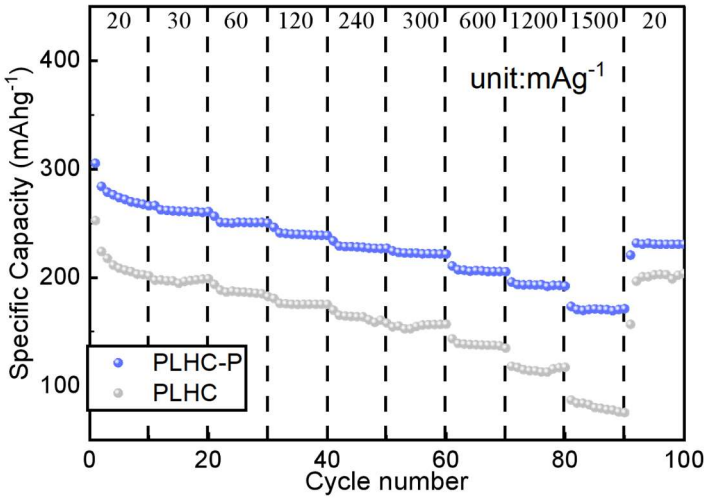

Fig. 6 Rate performance.

The great performance of PLHC-P is attributed to the modification of phosphoric acid. First, the optimized porous structure with abundant closed pores effectively accommodates volume expansion during repeated sodiation/desodiation, mitigating mechanical degradation [19]. Second, the expanded interlayer spacing (0.384 nm) facilitates rapid Na^+ diffusion and reduces structural stress [24]. Third, the introduction of phosphorus doping enhances electronic conductivity and stabilizes the electrode/electrolyte interface [31]. The reduced oxygen-containing functional groups also minimize irreversible side reactions, contributing to the high Coulombic efficiency observed throughout cycling.

ISSN: 2414-1895 DOI: 10.6919/ICJE.202604_12(4).0044

3.3 Discussion on Structure-performance Relationship

The comprehensive structural and electrochemical analyses reveal a clear structure-performance relationship for the wheat straw-derived hard carbon anodes. The phosphoric acid pretreatment plays a role in modulating the microstructure in three key aspects.

First, the enlarged interlayer spacing in PLHC-P facilitates more efficient Na^+ intercalation and deintercalation. The larger d-spacing reduces the diffusion barrier for sodium ions, which is particularly beneficial at high current densities where kinetics become rate-limiting.

Second, the increased structural disorder and reduced graphitization degree in PLHC-P, evidenced by the broader XRD peaks, preserve abundant defects and active sites for sodium storage. These defect sites can serve as additional adsorption sites for sodium ions, contributing to the higher reversible capacity observed in PLHC-P across all current densities.

Third, the successful incorporation of phosphorus doping and the reduction of oxygen-containing functional groups synergistically improve the electrochemical performance. Phosphorus doping enhances electronic conductivity and introduces additional active sites, while the reduced oxygen content minimizes irreversible side reactions during the initial sodiation process, contributing to the high Coulombic efficiency. The combination of these structural advantages enables PLHC-P to achieve both high capacity and excellent rate capability, outperforming the pristine PLHC anode.

4. Conclusion

In summary, we have successfully developed a simple phosphoric acid pretreatment strategy to regulate the microstructure of wheat straw-derived hard carbon for high-performance sodium-ion battery anodes. Systematic structural characterization reveals that phosphoric acid treatment effectively deconstructs the lignocellulosic structure, leading to an expanded interlayer spacing and successful phosphorus doping.

The optimized PLHC-P anode exhibits outstanding electrochemical performance:

- High reversible capacity of 300 mAh g^{-1} at 20 mA g^{-1}
- Superior rate capability, retaining 200 mAh g^{-1} at 300 mA g^{-1}
- Exceptional cycling stability with 92.9% capacity retention
- High Coulombic efficiency exceeding 99.5% throughout cycling

This work demonstrates that phosphoric acid-assisted structural engineering is an effective strategy for producing high-performance biomass-derived hard carbon anodes. PLHC-P has achieved significant improvements in initial coulombic efficiency, cycling stability, and rate performance.

Acknowledgments

Supported by the project of sci & tech of Zhongshan (2023A4011).

References

[1] N. Yabuuchi, K. Kubota, M. Dahbi, S. Komaba, Research development on sodium-ion batteries, Chem. Rev. 114 (2014) 11636–11682.

[2] J.Y. Hwang, S.T. Myung, Y.K. Sun, Sodium-ion batteries: present and future, Chem. Soc. Rev. 46 (2017) 3529–3614.

[3] Y. Cao, The opportunities and challenges of sodium ion battery, Energy Storage Sci. Technol. 9 (2020) 757.

[4] M. Sawicki, L.L. Shaw, Advances and challenges of sodium ion batteries as post lithium-ion batteries, RSC Adv. 5 (2015) 53129–53154.

[5] D.-L. Cheng, L.-C. Yang, M. Zhu, High-performance anode materials for Na-ion batteries, Rare Met. 37 (2018) 167–180.

[6] J. Wang, L. Xi, C. Peng et al., Recent progress in hard carbon anodes for sodium-ion batteries, Adv. Eng. Mater. 26 (2024) 2302063.

ISSN: 2414-1895 DOI: 10.6919/ICJE.202604_12(4).0044

[7] X. Chen, N. Sawut, K. Chen et al., Filling carbon: a microstructure-engineered hard carbon for efficient alkali metal ion storage, Energy Environ. Sci. 16 (2023) 4041–4053.

[8] D. Alvira, D. Antorán, J.J. Manyà, Plant-derived hard carbon as anode for sodium-ion batteries: a comprehensive review to guide interdisciplinary research, Chem. Eng. J. 447 (2022) 137468.

[9] X. Dou, I. Hasa, D. Saurel et al., Hard carbons for sodium-ion batteries: structure, analysis, sustainability, and electrochemistry, Mater. Today 23 (2019) 87–104.

[10] D. Saurel, B. Orayech, B. Xiao et al., From charge storage mechanism to performance: a roadmap toward high specific energy sodium-ion batteries through carbon anode optimization, Adv. Energy Mater. 8 (2018) 1703268.

[11] Q. Meng, Y. Lu, F. Ding et al., Tuning the closed pore structure of hard carbons with the highest Na storage capacity, ACS Energy Lett. 4 (2019) 2608–2612.

[12] C. Zhao, Q. Wang, Y. Lu et al., High-temperature treatment induced carbon anode with ultrahigh Na storage capacity at low-voltage Plateau, Sci. Bull. 63 (2018) 1125–1129.

[13] Y. Huang, Z. Tang, S. Zhou et al., Renewable waste biomass-derived carbon materials for energy storage, J. Phys. D: Appl. Phys. 55 (2022) 313002.

[14] J. Zhu, J. Roscoe, S. Chandrasekaran et al., Biomass-derived carbons for sodium-ion batteries and sodium-ion capacitors, ChemSusChem 13 (2020) 1275–1295.

[15] C.D.M. Saavedra Rios, L. Simonin, A.D. Geyer et al., Unraveling the properties of biomass-derived hard carbons upon thermal treatment for a practical application in Na-ion batteries, Energies 13 (2020) 3513.

[16] S. Zhou, Z. Tang, G. Jin et al., Understanding the relationship of closed pore structure in biomass-derived hard carbon with cellulose regulating strategy, Small 20 (2024) 2407341.

[17] Z. Huang, J. Huang, L. Zhong et al., Deconstruction engineering of lignocellulose toward high-plateau-capacity hard carbon anodes for sodium-ion batteries, Small 20 (2024) 2405632.

[18] S. Zhou, Z. Tang, Z. Pan et al., Regulating closed pore structure enables significantly improved sodium storage for hard carbon pyrolyzing at relatively low temperature, SusMat 2 (2022) 357–367.

[19] Z. Tang, R. Zhang, H. Wang et al., Revealing the closed pore formation of waste wood-derived hard carbon for advanced sodium-ion battery, Nat. Commun. 14 (2023) 6024.

[20] Z. Li, L. Ma, T.W. Surta et al., High capacity of hard carbon anode in Na-ion batteries unlocked by PO_x doping, ACS Energy Lett. 1 (2016) 395–401.

[21] P. Bai, Y. He, X. Zou et al., Elucidation of the sodium-storage mechanism in hard carbons, Adv. Energy Mater. 8 (2018) 1703217.

[22] M. Palanisamy, R. Perumal, V.G. Pol, Mesoporous weaved turbostratic nanodomains enable stable Na^+ ion storage, ACS Appl. Mater. Interfaces 14 (2021) 684–697.

[23] T. Xu, X. Qiu, X. Zhang, Y. Xia, Regulation of surface oxygen functional groups and pore structure of bamboo-derived hard carbon for enhanced sodium storage performance, Chem. Eng. J. 452 (2023) 139514.

[24] Y. Li, Y. Yuan, Y. Bai et al., Insights into the Na^+ storage mechanism of phosphorous-functionalized hard carbon as ultrahigh capacity anodes, Adv. Energy Mater. 8 (2018) 1702781.

[25] E.M. Lotfabad, J. Ding, K. Cui et al., High-density sodium and lithium ion battery anodes from banana peels, ACS Nano 8 (2014) 7115–7129.

[26] J. Deng, T. Xiong, H. Wang et al., Effects of cellulose, hemicellulose, and lignin on the structure and morphology of porous carbons, ACS Sustainable Chem. Eng. 4 (2016) 3750–3756.

[27] J. Zhao, X. He, W. Lai et al., Catalytic defect-repairing using manganese ions for hard carbon anode with high-capacity and high-initial-Coulombic-efficiency in sodium-ion batteries, Adv. Energy Mater. 13 (2023) 2300444.

[28] Q. He, H. Chen, X. Chen et al., Tea-derived sustainable materials, Adv. Funct. Mater. 34 (2024) 2310226.

[29] D. Wu, Z. Yao, X. Sun et al., Mussel-tailored carbon fiber/carbon nanotubes interface for elevated interfacial properties of carbon fiber/epoxy composites, Chem. Eng. J. 429 (2022) 132449.

[30] Z.-G. Liu, J. Zhao, H. Yao et al., P-doped spherical hard carbon with high initial coulombic efficiency and enhanced capacity for sodium ion batteries, Chem. Sci. 15 (2024) 8478–8487.

ISSN: 2414-1895 DOI: 10.6919/ICJE.202604_12(4).0044

[31] H. Zhao, J. Ye, W. Song et al., Insights into the surface oxygen functional group-driven fast and stable sodium adsorption on carbon, ACS Appl. Mater. Interfaces 12 (2020) 6991–7000.

[32] Y. Zheng, Y. Lu, X. Qi et al., Superior electrochemical performance of sodium-ion full-cell using poplar wood derived hard carbon anode, Energy Storage Mater. 18 (2019) 269–279.

[33] V.A. Agubra, J.W. Fergus, The formation and stability of the solid electrolyte interface on the graphite anode, J. Power Sources 268 (2014) 153–162.